

Electron Density and Temperature Decay in Mercury Afterglows

M. Sugawara and B. C. Gregory

Department of Physics, Trent University, Peterborough, Ontario, Canada

(Received 2 March 1970)

Average electron number density and electron-temperature measurements are presented for the mercury vapor afterglow in a hot-cathode cylindrical discharge tube at a pressure range where ambipolar diffusion predominates. The average electron number density is measured using cylindrical microwave cavities in the TM_{010} and dipole resonance modes. The electron temperature is measured by means of a time-resolving 3.0-GHz radiometer. Three pressure regions are identified: (1) $p_0 < 0.08$ Torr, where p_0/τ_n increases with p_0 , (2) $0.08 < p_0 < 0.18$ Torr, where p_0/τ_n is roughly constant, and (3) $0.18 \text{ Torr} < p_0$, where p_0/τ_n increases. Here p_0 and τ_n are the pressure reduced to 0°C and the density decay time constant, respectively. The work presented here is concerned mainly with the first two pressure regions. In the lowest pressure region, electron-temperature measurements in the afterglow under experimental conditions identical to those used for density measurements are used to determine after which point in time the electrons reach the neutral-atom temperature. This information, along with the density decay time constant, is used to predict a mobility of $0.21 \text{ cm}^2 \text{ V}^{-1} \text{ sec}^{-1}$ at 760 Torr for Hg^+ in mercury vapor at 443°K . This value is in good agreement with previous theoretical and experimental work. In the second pressure range, the electron-temperature measurements indicate that, after an initially rapid drop, a slow decay of electron temperature occurs from roughly 1050 to 600°K between 0.5 and 5 msec. In spite of this temperature change, the density decay curves were exponential over two decades. This curious observation, which has led previous workers to predict a constant electron temperature around 2000°K for periods of several milliseconds in the afterglow, has been explained by postulating that the ion mobility could vary over this period. The reasons for this assumption are given in the paper and involve Coulomb collisions which are very important in these experiments. The initially rapid electron-temperature decay occurring during the first 0.5 msec of the afterglow is pressure independent and is well explained by electron-ion elastic collisions. The slow electron temperature decay after 0.5 msec which occurs in the second pressure region is pressure dependent and is explained by a balance between energy gain from collisions of the second kind in the reaction $e + {}^3P_2 \rightarrow {}^3P_1 + e$ and losses due to electron-ion elastic collisions. A complete discussion of these processes is given and the neglect of other mechanisms justified.

I. INTRODUCTION

A great deal of experimental work has been carried out in afterglow plasmas to determine the mobilities of positive ions in their parent gases and to study other collisional processes. Measurements of the variation of the electron density in the afterglow of a pulsed discharge have yielded information concerning the ambipolar diffusion of charged particles and the recombination and conversion processes of positive ions.

Studies of the mercury afterglow have been carried out by Mierdel¹ using Langmuir probes, and by Dandurand and Holt² and Biondi³ using microwave techniques. In Refs. 1 and 2, the electrons were not in thermal equilibrium with the ambient mercury vapor. As a result, only qualitative remarks could be made concerning the processes occurring in the afterglow. Using a Langmuir probe in the afterglow at a reduced pressure (0°C) of $p_0 = 66 \text{ mTorr}$, Mierdel found that the

electron temperature decayed to 2200°K within 0.25 msec and remained at a substantially constant value of about 2000°K for 2.5 msec. However, it is known that electron collection by a probe in an active plasma will deplete electrons around the probe; this effect is especially notable in a pressure range where the electron mean free path is smaller than the size of the probe.⁴ In an afterglow plasma, the depletion is a very serious perturbation because of the absence of ionization, and distorts the voltage-current characteristic of the probe to yield apparent higher electron temperatures. Therefore, the use of a Langmuir probe in the afterglow for the measurement of electron density and especially for the measurement of electron temperature is somewhat doubtful. A simple calculation shows that a small probe with a ratio of $R/a=25$ (where R is the tube radius and a is the radius of a disc probe) may collect an appreciable fraction of the total number of electrons within the first 20 μsec of the afterglow.

Dandurand and Holt obtained the electron temperature in the afterglow from the measured electron-density decay time constant. Their results support Mierdel's.

In the first part of Biondi's experiment, helium was added as a recoil gas to bring the electrons into thermal equilibrium with the atoms in the afterglow plasma. Differentiating charged particle collisions with mercury vapor atoms from collisions with helium atoms, he obtained separately the ambipolar diffusion coefficients of Hg^+ and electrons in mercury atoms and helium atoms. In addition, from a study of the ionization produced by collisions of pairs of mercury metastable atoms, the diffusion coefficient of the metastable atoms (the 3P_2 state) was obtained. In the case of pure mercury, he estimated the electron temperature from the linear decay of the electron density. He found a value similar to Mierdel's.

The observation that the electron density decayed exponentially suggests that the coefficient of ambipolar diffusion remained substantially constant during the period of observation. Mierdel proposed that electrons gain energy from collisions of the second kind with metastable atoms and lose energy by inelastic collisions as well as elastic collisions. A balance between the gain and loss processes causes the essentially constant electron temperature. However, Biondi made two criticisms of their argument. First, the characteristic time constant of elastic recoil collisions with atoms is very much longer than the early electron-temperature decay time measured by Mierdel. Second, the fast electrons (~ 5 -eV energy) produced by collisions of the second kind would diffuse to the walls before losing appreciable energy by recoil collisions with atoms. He suggested that electrons produced in the afterglow by metastable-metastable collisions (electrons with initial energy of 0.5 eV will diffuse against the ambipolar space charge field and may reduce their average energy to about 0.3 eV, the value calculated from the measured electron-density decay time constant. However, in the pressure range of his experiment the mean lifetime of electrons is determined by diffusion and is of the order of milliseconds. Surely therefore, elastic recoil collisions with atoms would also be an important energy-loss mechanism in addition to diffusion cooling.

We have found that electron-ion collisions are the dominant electron energy-loss process in the afterglow under our experimental conditions. The present study is initiated by an attempt to measure reliable temperatures using a radiometer and to explain in detail the decay processes of electron density and energy in the afterglow.

II. PROCESSES IN THE AFTERGLOW

A. Decay of Electron Number Density

Previous study of afterglow plasmas in mercury vapor has shown that the principal processes governing the variation of the ion and electron densities with time are ambipolar diffusion of ions and electrons to the container walls, conversion of atomic to molecular ions, and recombination of the molecular ions with electrons. Biondi³ has shown that in the mercury afterglow plasma the conversion process of Hg^+ occurs by a three-body process of the form



The loss rate of the atomic mercury ions due to ambipolar diffusion and conversion is given by the differential equation

$$\frac{\partial n_i}{\partial t} = D_a \nabla^2 n_i - \beta n_i, \quad (2)$$

where n_i is the atomic ion number density, D_a is the ambipolar diffusion coefficient of the atomic ion species, and β is the conversion frequency.

The solution of this equation, when diffusion occurs in the fundamental mode alone, indicates an exponential decrease of the ion number density with time, with a decay time constant τ_n given by

$$1/\tau_n = (D_a/\Lambda^2) + \eta p_0^2. \quad (3)$$

Here Λ is the fundamental-mode characteristic diffusion length of the plasma, η is the rate coefficient for the three-body conversion process ($\beta = \eta p_0^2$), and p_0 is the value of the vapor pressure reduced to the standard temperature of 0°C. For the cylindrical discharge tube used in the present experiments, $\Lambda^2 = (R/2.405)^2 = 0.21 \text{ cm}^2$, where R is the tube radius (1.1 cm). Since the ambipolar diffusion coefficient is inversely proportional to the reduced pressure, it is more convenient to express Eq. (3) in terms of the product $D_a p_0 = D_{a1}$ (D_{a1} is the ambipolar diffusion coefficient at 1 Torr) as

$$p_0/\tau_n = D_{a1}/\Lambda^2 + \eta p_0^3. \quad (4)$$

The ambipolar diffusion coefficient D_{a1} and the conversion coefficient η may therefore, be determined by measuring τ_n at different vapor pressures and plotting the results in the form of p_0/τ_n against p_0 or p_0^3 .

The ambipolar diffusion coefficient D_a is related to the diffusion coefficients and mobilities of the ions and electrons by the relation

$$D_a = \frac{D_e \mu_i + D_i \mu_e}{\mu_e + \mu_i} \cong \mu_i \frac{kT_e}{e} \left(1 + \frac{T_i}{T_e} \right), \quad (5)$$

where D , μ , and T are the diffusion coefficient, mobility, and temperature, respectively, of each

particle, and subscripts i and e refer to ions and electrons. Thus measurements of D_a yield values of the ion mobilities when the ion and electron temperatures are known.

B. Decay of Electron Energy

The electron-energy decay in the afterglow is determined by the balance between energy gain and loss mechanisms. To interpret properly the observed electron-energy decay, it is desirable to know the electron velocity distribution. The electron energy is determined experimentally by the measurement of the plasma radiation temperature T_r which is equal to the electron temperature T_e if the electrons have a Maxwellian velocity distribution.^{5,6} The time constant τ_{ee} for energy relaxation by electron-electron interactions⁷ is a rough measure of the Maxwellianization time constant. This time constant is given by

$$\tau_{ee} = 2.59 \times 10^5 (U_e^3/n_e \ln \delta) \text{ sec.} \quad (6)$$

Here, U_e is the electron energy in eV, and $\delta = 1.24 \times 10^4 (T_e^3/n_e)^{1/2}$. As a typical example, for $n_e = 5 \times 10^{11} \text{ cm}^{-3}$ and $U_e = 0.5 \text{ eV}$, we obtain $\tau_{ee} = 2 \times 10^{-8} \text{ sec}$, which is shorter by about four orders of magnitude than the characteristic time constant of the early electron-energy decay and of the electron-density decay. We therefore expect that electrons have approximately a Maxwellian velocity distribution in the afterglow, and that our measured radiation temperatures T_r are very close to the electron temperatures T_e . We will show experimentally that this is true in the active discharge.

Mechanisms which can act to increase the electron energy are (a) collisions of the second kind involving a free electron and a mercury atom in a metastable state and (b) ionizing collisions between two metastable atoms (only the 3P_2 state of 5.43-eV excitation energy can ionize) producing 0.44-eV electrons. However, in the late afterglow, where the average electron energy is about 0.1 eV in our experiment, the density of these electrons is very small and their contribution to the increase of electron energy can be neglected compared to the energy gain obtained from collisions of the second kind between electrons and metastables.

Ambipolar diffusion generally tends to cool the electrons. In any case, its direct cooling effect on the electrons may be neglected for the conditions of our experiment. This can be seen from a comparison of the electron-density decay time constant τ_n with the collisional energy relaxation time constant of electrons. In our experimental conditions, the value of τ_n is approximately ten times the energy relaxation time constant.

For the electron densities involved in this experiment, we will show experimentally that electron-ion elastic recoil collisions are dominant. The effect of inelastic collisions with ground-state atoms may be neglected, but those with metastable atoms must be taken into account. In summary, only energy gain from collisions of the second kind is important, and energy losses are due to elastic recoil collisions with atoms and ions and inelastic collisions with metastable atoms.

With these approximations, the average electron energy $\frac{3}{2}eU_e$ in an axially uniform afterglow plasma with no applied electric field can be written

$$\begin{aligned} \frac{d}{dt} (\frac{3}{2}eU_e) = & H - J - \bar{v}_e \{ K_{e1} [\frac{3}{2}e(U_e - U_g) n_g \bar{q}_{eg} \\ & + \frac{3}{2}e(U_e - U_i) n_i \bar{q}_{ei}] \}, \end{aligned} \quad (7)$$

where the symbols are defined as follows: n_g is the number density of atoms in the ground state, n_i is the number density of ions, \bar{v}_e the average electron velocity, K_{e1} the elastic energy-loss factor $= \frac{8}{3} (m_e/M) [1 + (U_{g,i}/U_e)]$, where m_e and M are the electron and atom masses, respectively, U_g is the ground-state atomic energy in eV, U_i the ion energy in eV (approximately equal to U_g), \bar{q}_{eg} the average momentum-transfer collision cross section of electrons with the ground-state atom, and \bar{q}_{ei} is the average Coulomb collision cross section at an electron energy U_e . The first term H on the right-hand side of Eq. (7) represents the energy gain due to collisions of the second kind. The second term J is the inelastic collision term. The third and fourth terms represent the energy losses due to the recoil collisions with atoms and ions, respectively.

III. EXPERIMENTAL METHODS AND RESULTS

A. Electron-Density Decay

Experiments were carried out in a Pyrex discharge tube of inner diameter 2.2 cm having a mercury finger reservoir heated to the desired temperatures. Details of the tube construction and processing are given in Ref. 8. The discharge tube itself was kept at 170 °C. Current pulses were of 0.5–2.0 A and 50 μsec duration. The pulse repetition frequency was varied from 50 to 100 Hz, depending on the vapor pressure. The criterion here was that the density should be negligibly small halfway between the current pulses. The vapor pressure was varied from 0.02 to 0.65 Torr by controlling the temperature of the finger.

The average number density of electrons was measured with a perturbation TM_{010} mode cavity.^{9,10} A dipole mode cavity⁸ was used to verify the TM_{010} mode cavity measurements, and was found to be especially useful in the very early afterglow. Data

shown in this paper were taken with the TM_{010} mode cavity.

Semilogarithmic graphs of the average electron number density as a function of time in the afterglow (see Figs. 1 and 2) were linear over two orders of magnitude except for the lowest pressure measurements of Fig. 1. The observation that the electron density decayed exponentially is not only evidence for an exponential loss process, but also suggests that the value of D_a is substantially constant during the period of observation. Results of measurements of p_0/τ_n are shown in Fig. 3 as a function of vapor pressure. From this figure it can be seen that the curve may be separated in the following three pressure regions: (1) $p_0 < 0.08$ Torr, where p_0/τ_n increases with p_0 , (2) $0.08 < p_0 < 0.18$ Torr, where p_0/τ_n is almost constant, and (3) 0.18 Torr $< p_0$, where p_0/τ_n increases steeply.

B. Electron-Energy Decay

The electron-energy decay in the afterglow was measured by means of a time-resolving 3.0-GHz radiometer of the type first described by Ingraham and Brown.¹¹ The time resolution of our radiometer is 2 μ sec. A block diagram of this device is given in Fig. 4. The theory of this technique for measuring the electron temperature is ade-

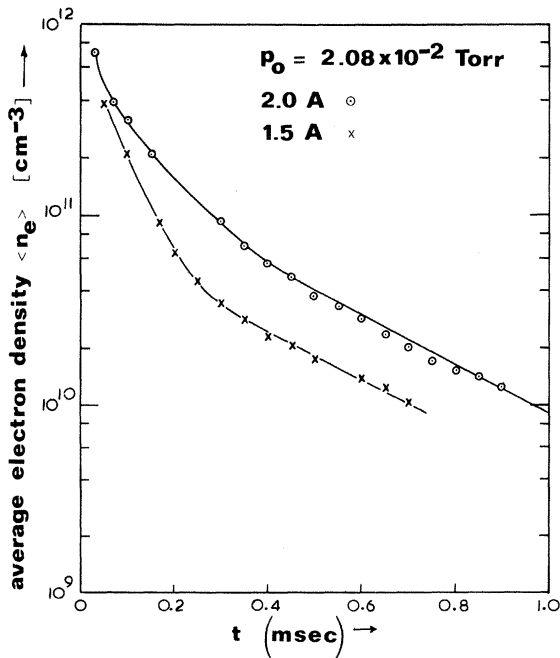


FIG. 1. Typical electron-density decay curves at $p_0 = 2.08 \times 10^{-2}$ Torr. From the linear portion of the curves, $\tau_n = 0.36$ msec.

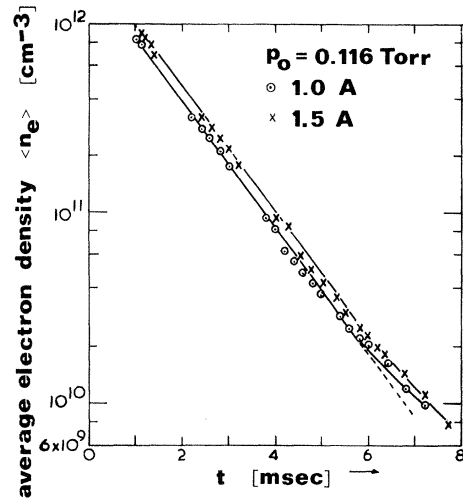


FIG. 2. Typical electron-density decay curves at $p_0 = 0.116$ Torr. From the slope, $\tau_n = 1.22$ msec.

quately described in Ref. 6.

To ensure that the radiometer results are dependable we have measured the absorptivity of the plasma column at the center frequency (3.0 GHz) in the afterglow and the reflections and attenuations in the coaxial lines, the waveguide, and the circulator. The effect of these various reflections and absorptions on the radiometer balance condition was taken into account in a detailed analysis. Finally, the radiometer results were compared with the Langmuir-probe temperature measurements (see Sec. IV B). We are confident that the radiometer is performing correctly for the measurements described in this paper.

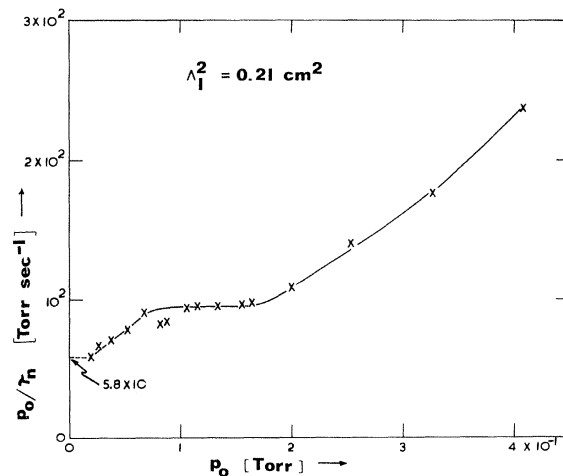


FIG. 3. p_0/τ_n versus p_0 .

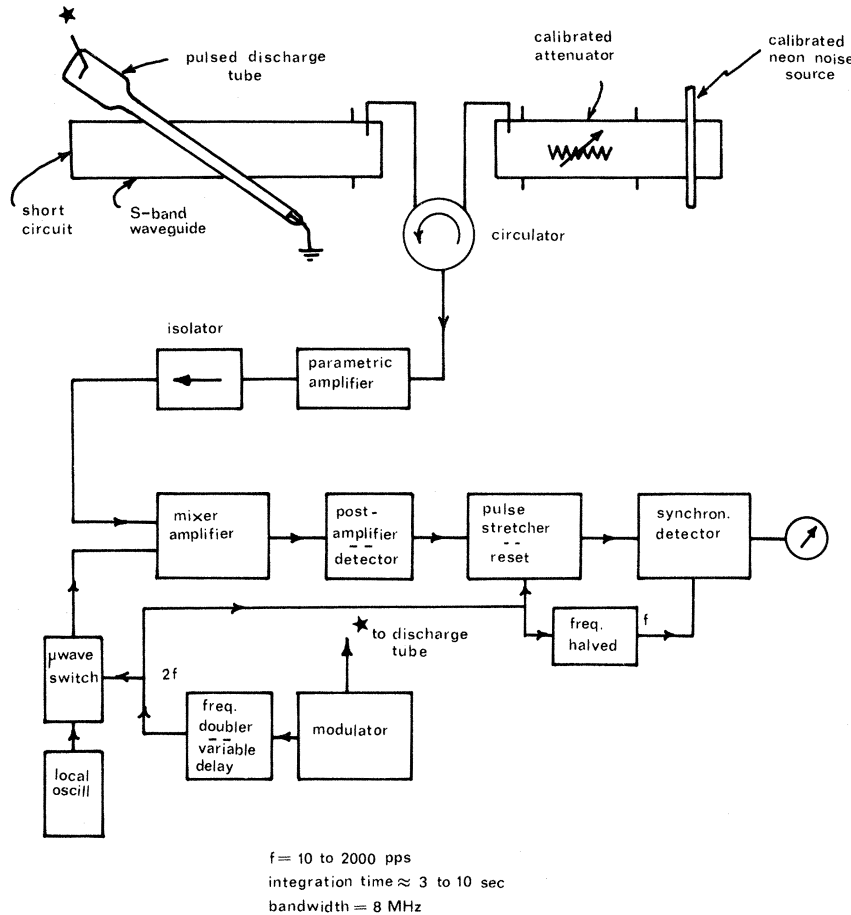


FIG. 4. The 3.0-GHz time-resolving radiometer.

Measurements of the electron energy decay have been made in the pressure ranging from 2.08×10^{-2} to 0.253 Torr. Typical data taken in the first pressure region (see Sec. III A) and the second pressure region are shown in Figs. 5 and 6, respectively.

It is found from these observations that the electron-energy decay curve can be separated into two parts, one of fast energy decay and another of relatively slow energy decay. The electron energy decays quickly within about 0.5 msec, irrespective of the vapor pressure. In the second region, the energy decays more gradually to the oven temperature of 443 °K (see Fig. 6).

IV. DISCUSSION

A. Electron-Density Decay

Initially we shall discuss the cavity method used to measure the average electron density. As a result of the electron collision frequency there may be a correction needed in the formula relating electron density to the change in resonant frequen-

cy of the cavity. The frequency shift taking into account collisions is given by¹²

$$\frac{\Delta\omega}{\omega_0} = A \frac{\omega_p^2}{\omega^2} \frac{1}{1 + (\nu/\omega)^2}, \quad (8)$$

where $\Delta\omega$ is the frequency shift due to the presence of plasma, and ω_0 , ω_p , ν , and A are, respectively, the resonant frequency without plasma, the average plasma frequency, the electron collision frequency with other particles, and a geometrical factor. Using Adler and Margenau's data¹³ for the elastic collision probability of electrons in mercury and the classical formula⁷ for electron-ion Coulomb collisions, we estimate ν/ω to be less than 0.1 over the density pressure range in this work. Since this experiment is more concerned with exact absolute density values, the collisional correction factor has been neglected. We have used a theory for the TM_{010} mode⁹ which takes into account the effects of the cavity end holes as well as the thickness of the glass tube containing the plasma.

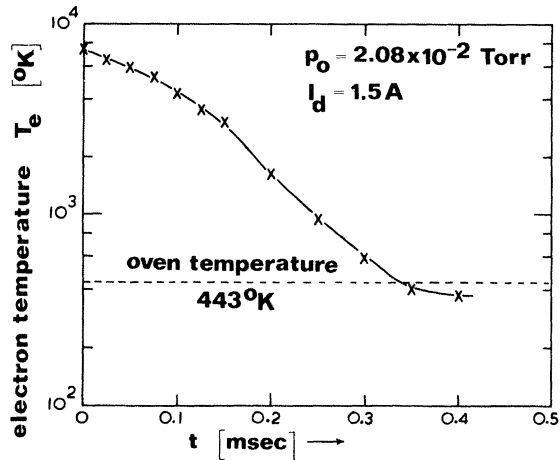


FIG. 5. Electron-temperature decay at $p_0 = 2.08 \times 10^{-2}$ Torr.

It is of considerable importance in discussing the expected behavior of mercury vapor afterglows to consider the effect on the plasma decay of small impurity concentrations. The reaction of mercury ions with impurities (probably a charge-exchange process) is an additional loss process and causes an increase in the rate of decay above that due to diffusion and conversion. No data for charge exchange between Hg^+ and other gas molecules (N_2 or O_2) are available. However, atoms having a lower ionization potential have a larger cross section¹⁴ of the symmetrical resonant charge exchange and because this cross section is much larger than that for nonsymmetrical charge-exchange collisions, we expect the effect of impurities on the motion of Hg^+ ions to be negligible. In addition, since the total collision cross section of electrons with mercury atoms is more than an order of magnitude larger than that of collisions with the molecular gases N_2 or O_2 , the effect of impurities on the motion of electrons is probably negligible. Using a spectroscope (Spex-1700-II), no detectable lines of impurity gases were observed.

The requirements to ensure ambipolar diffusion in the afterglow, that the Debye length and mean free paths be much smaller than the tube dimensions, have been satisfied in the pressure and electron-density range of this experiment.

Studying Figs. 1 and 5, taken at $p_0 = 2.08 \times 10^{-2}$ Torr, it can be seen that in the linear portion of the semilog plots of the electron density, electrons have reached thermal equilibrium with the oven temperature, which is approximately equal to the atomic temperature, $T_e = T_g$. Using Eq. (4) with the measured value of $p_0/\tau_n = 5.8 \times 10$ Torr sec^{-1} and setting $\eta = 0$, we obtain

$$D_{a1}/\Lambda^2 = 5.8 \times 10. \quad (9)$$

This value yields $\mu_i = 0.21 \text{ cm}^2 \text{ V}^{-1} \text{ sec}^{-1}$ at $p_0 = 760$ Torr for the mobility of Hg^+ ions at 443°K. Since the vapor pressure is low, the mercury ions are considered to be atomic. Our mobility value compares well with the measured values of 0.29 obtained by Mierdel,¹ 0.22 obtained by Biondi,³ and the most recent measurement of 0.24 ± 0.03 obtained by Kovar.¹⁵ It also lies between the two theoretical values obtained by Dalgarno¹⁶ and McConnel *et al.*¹⁷

As the pressure is increased in the first region, p_0/τ_n increases (Fig. 3) and the long slowly-decaying electron-temperature tail seen clearly in Fig. 6 gradually increases above the oven temperature.

In the second pressure region, the measurements of the electron-density decay and the electron-energy decay are shown in Figs. 2 and 6. The two curves in Fig. 6 coincide. Because p_0/τ_n is a function only of electron and ion temperatures as well as ion mobility, identical afterglow electron temperatures implies identical decay time constants, a fact well verified in Fig. 3 for the two pressures concerned.

Over the time range of the electron-density decay measurements (Fig. 2), the electron temperature decays from 1050 to 600°K (Fig. 6), implying that the slope of the density decay curve might be expected to change by a factor of $(1050 + 443)/(600 + 443) \approx 1.4$. However, the value of ion mobility μ_i is not necessarily constant during the afterglow. In fact, the value of μ_i at a earlier times may be smaller than that later on in the afterglow. There seem to be two possibilities to explain this

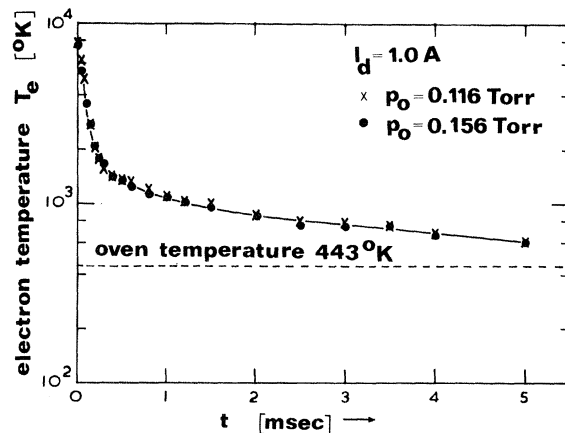


FIG. 6. Electron-temperature decay at $p_0 = 0.116$ Torr and $p_0 = 0.156$ Torr.

hypothesis.

First of all, the ion temperature in the afterglow may vary with time because in the early afterglow, where the electron density and temperature are high, the ions may gain energy from the electrons by frequent Coulomb collisions (see Sec. IV B). The ion energy at earlier times is probably higher than that at later times. Theories^{16,17} predict that the value of μ_i at a higher ion energy is smaller than that at a lower ion energy. Although the value of D_{a1} is a product of μ_i and $(U_e + U_i)$, and in spite of the fact that the effect of high ion energies on both terms is opposite, increasing ion energy does decrease D_{a1} .

A second possibility, which would contribute to the above phenomenon, is the momentum loss of drifting ions owing to interaction with electrons and stationary ions. This effect is also important in the afterglow, because there the Coulomb collisions are more important than collisions with atoms. This effect would also lower the value of μ_i . Therefore, to evaluate the electron temperature from the linear density decay curve^{1,3} may be misleading and will result in higher electron temperatures.

The third pressure region, where the value of p_0/τ_n increases steeply with p_0 , suggests that loss mechanisms other than ambipolar diffusion loss are taking place. This process is explained by the three-body conversion process of the ions, $\text{Hg}^+ + 2\text{Hg} \rightarrow \text{Hg}_2^+ + \text{Hg}$. The rate coefficient of this process was obtained by Biondi.³ Although the present paper is not concerned with this pressure region, we have checked the linear relationship between $(p_0/\tau_n - D_{a1}/\Lambda^2)$ and p_0^3 .

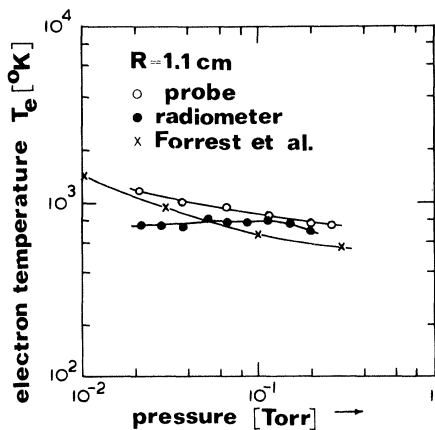


FIG. 7. Electron temperature versus pressure in the active discharge, theory, and experiment (probe and radiometer).

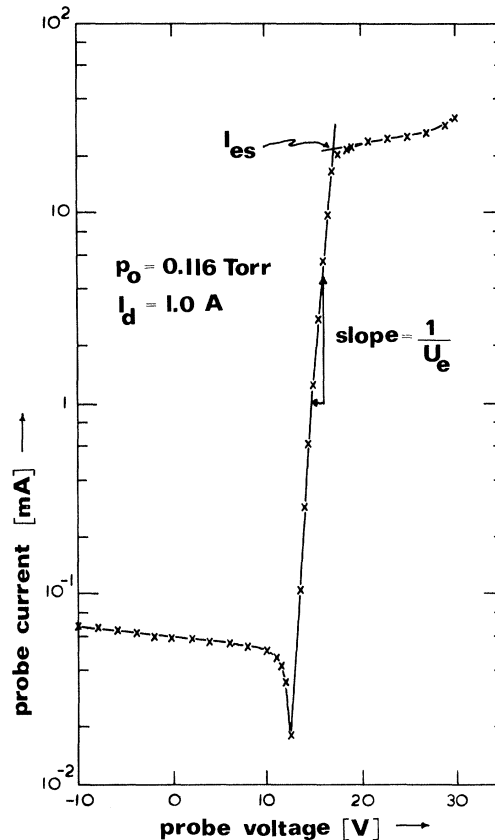


FIG. 8. Voltage-current Langmuir-probe characteristic.

B. Electron-Energy Decay

To verify the radiometer measurements, a comparison with a Langmuir probe was made in the active discharge (Fig. 7). Figure 8 shows a probe characteristic. Agreement between these two methods is good except for lower pressures. It has been found¹⁸ that in the mercury vapor pressures range from 10^{-3} to 10^{-2} Torr, where the mean free path of electrons is greater than the tube dimensions, the radiation temperature was nearly half the electron temperature obtained by means of a Langmuir probe. This has been explained using a noise diode theory which is justified by the similarity between the plasma wall sheath and the diode. This theory may be applicable to the lowest pressure situations in our experiment.

Applying such a correction factor to the radiation temperature in the active discharge it becomes evident that in Fig. 5 the electron temperature approaches the oven temperature at $t \approx 0.3 - 0.4$ msec. As a further comparison, a theoretical prediction obtained by Forrest *et al.*,¹⁹ taking into account a two-step ionization process (applicable

to our experimental conditions) is shown in Fig. 7. It shows good agreement with the Langmuir-probe data.

As pointed out in Sec. III B, the electron temperatures decay very quickly in the first 0.5 msec (hereafter region I) independently of the vapor pressure over the whole pressure range in this experiment. This simply implies that the initial temperature decay is independent of the presence of atoms. To explain this phenomenon we propose that diffusion cooling and recoil collisions with atoms are negligible compared to recoil collisions with ions. It can be seen that after the initial decay the electron temperature at higher pressures decays rather slowly to oven temperature. This region of slow decay shall be designated region II. The experimental results suggest that the heating mechanism of the electrons depends on the atomic density and is probably related to the diffusion coefficient of the metastable mercury atoms.

In order to determine the effect of ion recoil collisions, let us retain only the ion recoil collision term in Eq. (7).

Using $K_{ei} = \frac{2}{3} (m_e/M)(1 + U_i/U_e)$,

$$\frac{d}{dT} (eU_e) = -\frac{8}{3} \frac{m_e}{M} e(U_e - U_i) \frac{3_e 63 n_i}{T_e^{3/2}} \ln \delta, \quad (10)$$

where $\delta = 1.24 \times 10^4 (T_e^3/n_e)^{1/2}$, n_e is in cm^{-3} , and T_e in $^\circ\text{K}$. Using $kT_e = eU_e$, $kT_i = eU_i$, and $n_i = n_e$, Eq. 10 becomes,

$$dT_e/dt = -2.8 \times 10^{-5} \ln \delta (n_e/T_e^{3/2})(T_e - T_i). \quad (11)$$

Since $\ln \delta$ is a weak function of T_e and n_e , we set $\ln \delta$ constant and assume that $n_e = n_{e0} e^{-t/\tau_{n1}}$ (where n_{e0} is the value of n_e extrapolated to $t=0$ in the early linear part of the electron-density decay). The solution of Eq. (11) is, therefore,

$$\begin{aligned} & \frac{2}{3} (T_{e0}^{3/2} - T_e^{3/2}) + 2T_i (T_{e0}^{1/2} - T_e^{1/2}) + T_i^{3/2} \\ & \times \ln \left| \frac{T_{e0}^{1/2} - T_i^{1/2}}{T_e^{1/2} - T_i^{1/2}} \frac{T_e^{1/2} + T_i^{1/2}}{T_{e0}^{1/2} + T_i^{1/2}} \right| \\ & = 2.8 \times 10^{-5} \tau_{n1} \ln \delta n_{e0} (1 - e^{-t/\tau_{n1}}), \end{aligned} \quad (12)$$

where T_{e0} is the value of T_e at $t=0$. Dipole cavity-density measurements were possible close to the time origin. These measurements, obtained at $p_0 = 0.116$ Torr and $I_d = 1.0$ A (hereafter we will discuss this pressure case), show an increase in slope at $t \cong 1$ msec, similar to that shown in the curves of Fig. 1. Such measurements were used to extend the TM_{010} cavity results to 0.4 msec from which the value of τ_{n1} and n_{e0} were obtained.

Employing the extrapolated value of $n_{e0} = 8.6 \times 10^{12} \text{ cm}^{-3}$, $\tau_{n1} = 0.39$ msec, $T_{e0} = 7800$ $^\circ\text{K}$, $T_i = 443$ $^\circ\text{K}$, and $\ln \delta = 9.0$ (value at $t=0$), we calculate T_e in Eq. (12) as shown in Fig. 9. The agreement

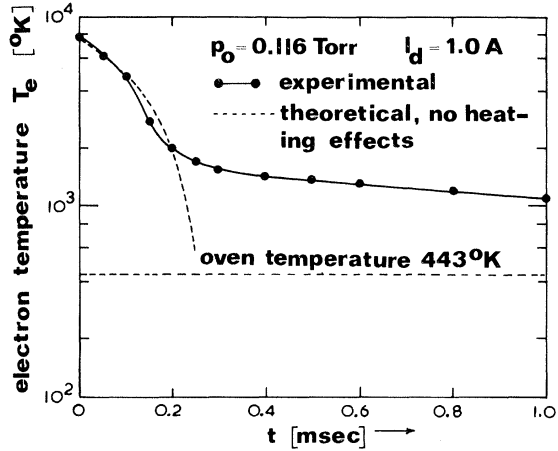


FIG. 9. Electron-temperature decay at $p_0 = 0.116$ Torr. The time scale is enlarged five times that of Fig. 6. Experiment and theory.

is satisfactory for region I, where we have verified that the energy gain mechanisms are much smaller than the electron-ion recoil loss process. The theoretical curve departs from the measured curve at about $t = 0.2$ msec, after which the heating mechanism, later shown to be collisions of the second kind with metastable atoms, becomes important.

The important heating collisions with metastable atoms are

- (i) $e + {}^3P_2 \rightarrow {}^3P_1 + e$, $\Delta U_m = 0.57$ eV,
- (ii) $e + {}^3P_2 \rightarrow {}^1S_0 + e$, $\Delta U_m = 5.43$ eV, (13)
- (iii) $e + {}^3P_1 \rightarrow {}^1S_0 + e$, $\Delta U_m = 4.86$ eV.

Collisions of the second kind between electrons and metastables remove electrons from one region of energy U , $U + \Delta U$, to another region $U + \Delta U_m$, $U + \Delta U_m + \Delta U$, where ΔU_m is the energy gain due to the collisions of the second kind. The electrons energized by collisions of the second kind [(ii) and (iii)] will tend to be Maxwellianized by electron-electron collisions in a characteristic time of 3.3 μsec [Eq. (6) with $n_e = 10^{11} \text{ cm}^{-3}$ and $U_e = 5.43$ eV]. Using the relationship $\lambda_{ei} = \bar{v}_e / \nu_{ei}$, where \bar{v}_e and λ_{ei} are, respectively, the mean velocity of electrons and the mean free path of electron-ion collisions, λ_{ei} is estimated as 4.7×10^2 cm for these high-energy electrons. Therefore, the lifetime of this high-energy group will be determined by free diffusion to the wall owing to electron-atom collisions and not by ambipolar diffusion. Assuming that the radial distribution of these electrons is in the form of the zeroth-order Bessel function, us-

ing the approximate formula $D_e = \frac{1}{3}\bar{v}_e\lambda_{ea}$ (where λ_{ea} is the mean free path for electron-atom collisions), and using Brode's data²⁰ for λ_{ea} , we obtain a diffusion time constant for these electrons (Λ^2/D_e) of 2×10^{-8} sec. Therefore, these high-energy electrons will diffuse out of the discharge before losing energy and attaining a Maxwellian distribution, and the energy-gain contribution from these high-energy electrons will be negligible.

The only important energy gain will be the process (i) in Eq. (13). The collisions of the second kind between an electron and a mercury metastable atom 3P_2 producing a 3P_1 metastable release 0.57 eV of energy to the electron and have a cross section maximum of 4.7×10^{-15} cm².²¹ The inverse process whereby the 3P_1 state is converted into the 3P_2 state through an inelastic collision with an electron should also be included. For electron temperatures below 2000 °K, the inverse process will be less than a 10% correction, assuming the 3P_1 resonance state density to be no greater than the 3P_2 metastable density, a fact which has been demonstrated by Kenty²¹ in a steady discharge. Retaining the recoil electron-ion and electron-atom collisions and collisions of the second kind between electrons and 3P_2 metastables in Eq. (7), we obtain

$$\left(\frac{d}{dt}\right) \frac{3}{2}eU_e = 0.57e\bar{v}_en_m\bar{q}_m - \bar{v}_e \frac{3}{2}e \\ \times (U_e - U_i)(n_i\bar{q}_{ei} + n_g\bar{q}_{eg}), \quad (14)$$

where \bar{q}_m is the mean cross section of electrons of collisions of the second kind with the 3P_2 state resulting in transfer to the 3P_1 state.

Considering that the deexcitation collision process of the 3P_2 state is small compared to its diffusion loss in the afterglow, the decay of the 3P_2 metastable density n_m is given by

$$n_m = n_{m0}e^{-t/\tau_m}, \quad (15)$$

where n_{m0} and τ_m are the initial density of metastables and their diffusion time constant, respectively. Using the measured value of the diffusion coefficient $D_m = 3.6 \times 10^2$ cm² sec⁻¹ at $p_0 = 0.116$ Torr for the 3P_2 metastables,³ and assuming that the radial distribution of the 3P_2 state is the zeroth-order Bessel function, we obtain $\tau_m = 0.6$ msec.

In region II of the electron-energy decay, the electron density decays exponentially as $n_i = n_e = n_{e0}e^{-t/\tau_{n2}}$, where n_{e0} and τ_{n2} are, respectively, the electron density extrapolated to $t=0$ in Fig. 2 and the decay time constant of the electron density ($\tau_{n2} = 1.22$ msec). It has been checked that even in the late afterglow (for example, $t = 3.7$ msec, where $n_e = 10^{11}$ cm⁻³) Coulomb collisions dominate, and therefore the term $n_g\bar{q}_{eg}$ is neglected in Eq. (14).

Since the electron-temperature dependence of \bar{q}_{ei} is T_e^{-2} and that of \bar{q}_m is approximately T_e^{-1} ,²¹ the energy dependence of $\bar{v}_e\bar{q}_m$ and of $\bar{v}_e(U_e - U_i)\bar{q}_{ei}$ with T_e are similar. Considering that the decay time constant τ_m is nearly half τ_{n2} , one might expect the energy decay rate to be much slower than the decay rate of the metastable density. This may explain the slow decay of the electron energy in region II.

In order to discuss the possibility of electron heating due to collisions of the second kind, the metastable density in the active discharge should be known. There are two approximate estimates for this quantity: one using the Boltzmann population and the other using the direct collisional excitation from the ground state.

If there were thermal equilibrium between the 3P_2 state and free electrons at temperature T_e , the population would be given by

$$n_{m0} = n_g(g_m/g_g)e^{-U_m/U_e}, \quad (16)$$

where n_g is the concentration of atoms in the ground state (about 4.1×10^{15} cm⁻³ at 0.116 Torr), and g_g and g_m are the statistical weights of the normal atom (= 1) and the 3P_2 atom (= 5), respectively, and U_m is the excitation potential of this metastable state (5.43 eV). For U_e the value 0.74 eV is used, based on probe measurements (Fig. 8). The population as calculated by Eq. (16) is $n_{m0} = 1.4 \times 10^{13}$ cm⁻³. In a steady discharge, it was found by Kenty²¹ that the populations of the 6^3P states saturated around 100 mA. He found that the use of the Boltzmann population was a reasonable estimate for the population ratio of the two metastable levels but gave absolute values which were roughly five times larger than those found experimentally.

We know that, in the electron-density region studied in this experiment, the metastable atoms and the free electrons are far from local thermal equilibrium²² and that, within the pulse length of 50 μsec, equilibrium of the metastable population may not be reached because the diffusion time constant of the 3P_2 atoms (0.6 msec) is much longer than the pulse length of the active discharge. Therefore, our second estimate involves calculating the direct excitation to the 3P_2 state. Assuming that the 3P_2 atoms are

$$\frac{dn_{m0}}{dt} = \left(\frac{2e}{m_e}\right)^{1/2} n_{e0}n_g \int_{U_m}^{\infty} F(U)U^{1/2}Q_m(U)dU, \quad (17)$$

where $F(U)$ is the Maxwellian energy distribution of electrons, U (eV) is the electron energy, and $Q_m(U)$ is the excitation cross section from the ground state to the 3P_2 state. Approximating the measured collision cross section²¹ by an analytical

function and integrating Eq. (17) numerically, we find dn_{m0}/dt for electrons of $U_e = 0.74$ eV to be

$$dn_{m0}/dt = n_{e0}n_g 5.77 \times 10^{-11}. \quad (18)$$

Substituting $n_g = 4.1 \times 10^{15}$ cm⁻³ and $n_{e0} = 8.6 \times 10^{12}$ cm⁻³, we obtain $dn_{m0}/dt = 1.24 \times 10^{18}$ cm⁻³ sec⁻¹. Assuming that the metastable population increases linearly with time during the breakdown pulse and neglecting deexcitation collisions and diffusion loss of the ³P₂ state, we obtain $n_{m0} = 6 \times 10^{13}$ cm⁻³, which is four times that obtained by the Boltzmann population calculation.

To verify our explanation of the slow electron-energy decay, the ratio of the first to the second term in Eq. (14),

$$\text{Ratio} = \frac{0.38 \bar{q}_m n_{m0} e^{-t/\tau_m}}{(U_e - U_i) \bar{q}_e n_{e0} e^{-t/\tau_n}}, \quad (19)$$

is calculated. Again, approximating the collision cross section for collisions of the second kind q_m by an analytical function and computing the average

cross section for Maxwellian electrons, we obtain a value for \bar{q}_m of 4×10^{-15} cm² at $U_e = 0.06$ eV (the electron temperature at $t = 3.7$ msec in Fig. 6). Substituting the electron density $n_{e0} = 1.7 \times 10^{12}$ cm⁻³ obtained by extrapolating the linear portion of Fig. 2 to $t = 0$ and the other values obtained above into Eq. (19), the ratio works out to be about 6.8.

This result may seem surprising, since it implies that the electron temperature would in fact, increase. We stress, however, the approximate nature of our calculations and, in particular, point out that we have used a value of n_{m0} which is 20 times Kenty's measured value. It can, nevertheless, be concluded that the heating mechanism due to collisions of the second kind is highly probable.

ACKNOWLEDGMENTS

Research Grant Nos. A-3157 of the National Research Council of Canada and 9510-54 of the Defence Research Board of Canada are gratefully acknowledged.

-
- ¹G. Mierdel, Z. Physik 121, 574 (1943).
²P. Dandurand and R. B. Holt, Phys. Rev. 82, 868 (1951).
³M. A. Biondi, Phys. Rev. 90, 730 (1953).
⁴J. F. Waymouth, Phys. Fluids 7, 1843 (1964).
⁵G. Bekefi and S. C. Brown, J. Appl. Phys. 32, 25 (1961).
⁶G. Bekefi, *Radiation Processes in Plasmas* (Wiley, New York, 1966).
⁷J. L. Delcroix, *Plasma Physics* (Wiley, New York, 1968), Vol. 2.
⁸B. C. Gregory, Can. J. Phys. 44, 2615 (1966).
⁹B. C. Gregory, Can. J. Phys. 46, 2281 (1968).
¹⁰P. Lukac, J. Phys. D 1, 1495 (1968).
¹¹J. C. Ingraham and S. C. Brown, Phys. Rev. 138, A1015 (1965).
¹²M. A. Heald and C. B. Wharton, *Plasma Diagnostics with Microwaves* (Wiley, New York, 1965).
¹³F. P. Adler and H. Margenau, Phys. Rev. 79, 970 (1950).
¹⁴J. B. Hasted, *Physics of Atomic Collisions* (Butterworths, London, 1964).
¹⁵F. R. Kovar, Phys. Rev. 133, A681 (1964).
¹⁶A. Dalgarno, Phil. Trans. Roy. Soc. London A250, 426 (1958).
¹⁷J. C. McConnell and B. L. Moiseiwitsch, J. Phys. B 2, 821 (1969).
¹⁸H. Prinzler, in *Proceedings of the Eighth International Conference on Phenomena in Ionized Gases* (Springer-Verlag, Vienna, 1967).
¹⁹J. R. Forrest and R. N. Franklin, J. Phys. B 2, 471 (1969).
²⁰R. B. Brode, Rev. Mod. Phys. 5, 257 (1933).
²¹C. Kenty, J. Appl. Phys. 21, 1309 (1950).
²²R. W. P. McWhirter, in *Plasma Diagnostics Techniques*, edited by R. H. Huddleston and S. L. Leonard (Academic, New York, 1965).